Altered immune and treatment response gene expression signatures among poverty-exposed children with B-cell acute lymphoblastic leukemia

Amy Guillaumet-Adkins,[1,2*] Elnaz Mirzaei Mehrabad,[3*] Noori Sotudeh,[1°] Sayalee Potdar,[1] Tushara Vijaykumar,[4] Monica Nair,[4] Valeriya Dimitrova,[1] Julia Frede,[4] Yana Pikman,[1,5,6] Marian Harris,[6,7] Andrew E. Place,[1,5,6] Lewis B. Silverman,[1,6,8] Jens G. Lohr,[3,4,6] Kira Bona[1,5,6] and Birgit Knoechel[1,3,5,6]

[1]Pediatric Oncology, Dana-Farber Cancer Institute, Boston, MA; [2]Broad Institute of Harvard and MIT, Cambridge, MA; [3]Huntsman Cancer Institute, Salt Lake City, UT; [4]Medical Oncology, Dana-Farber Cancer Institute, Boston, MA; [5]Department of Pediatrics, Boston Children's Hospital, Boston, MA; [6]Harvard Medical School, Boston, MA; [7]Department of Pathology, Boston Children's Hospital, Boston, MA and [8]Department of Pediatric Oncology, Columbia University, New York City, NY, USA

[°]*Current affiliation: AtlasXomics Inc., New Haven, CT, USA*

**AG-A and EMM contributed equally as first authors.*
[#]KB and BK contributed equally as senior authors.

Correspondence: B. Knoechel
birgit.knoechel@hci.utah.edu

K. Bona
kira.bona@childrens.harvard.edu

Received: October 7, 2025.
Accepted: April 28, 2026.
Early view: May 7, 2026.

https://doi.org/10.3324/haematol.2025.289187

©2026 Ferrata Storti Foundation
Published under a CC BY-NC license

Abstract

Children diagnosed with cancer typically receive standardized treatment regimens. Despite highly protocolized care, children living in poverty experience a greater risk of cancer relapse and higher mortality compared to their more affluent peers.[1,2] Acute lymphoblastic leukemia (ALL) is the most prevalent childhood cancer, and children with ALL exposed to poverty are more likely to experience early relapse.[3] Using single-cell RNA sequencing to analyze leukemic blasts and their microenvironment at diagnosis we found that poverty-exposed patients with standard-risk B-cell ALL (B-ALL) exhibit transcriptional signatures of steroid resistance at time of diagnosis. Additionally, we observed increased expression of inflammatory signatures in myeloid cells and reduced effector signatures in $CD8^+$ T cells in children with B-ALL living in poverty. Further investigation of the mechanisms underlying these associations may identify opportunities for risk-adapted therapeutic strategies to improve disease outcomes in pediatric ALL.

Introduction

Acute lymphoblastic leukemia (ALL) is the most common cancer of childhood, and 20% of children will suffer relapsed disease.[4-6] Despite improvements in therapy, only 50% of children who experience relapse will be long-term survivors.[6] Elucidating mechanisms of treatment resistance among populations at risk of relapse is essential to identify opportunities to improve pediatric ALL outcomes.

Early ALL relapse has been defined as relapse <36 months in complete remission[6] and is associated with particularly poor survival. Recent data have identified children exposed to poverty as a cohort at significantly higher risk of early relapse compared to unexposed children, despite uniform treatment on multi-center clinical trials. Among children who experienced leukemia relapse on a Dana-Farber ALL Consortium trial, 92% of relapses were early among poverty-exposed children compared to 48% relapses among unexposed children.[3,7] Additionally, recent publications have identified an association more broadly between proxied exposure to poverty and relapse and survival among children with ALL.[8,9]

Poverty is associated with profound health disparities in the US in diseases ranging from asthma to cancer.[10-12] While structural and sociobehavioral mechanisms underlying these associations - including access to care and adherence - have been delineated, they only partly explain observed disparities.[13] Emerging evidence suggests that gene-environment interactions may contribute to health outcome disparities in asthma, obesity and cardiovascular

disease - and help to explain the influence of stress on disease outcomes.[14,15] Early childhood exposure to poverty is associated with "toxic stress," defined by excessive activation of stress regulatory systems that impact neuroendocrine stress response axes including upregulation of the hypothalamic-pituitary-axis, elevated cortisol and cytokine responses to stress, and altered metabolism,[16-18] yet no studies have been performed to assess whether similar responses might be at play among children with cancer. Understanding the mechanistic pathways underlying these associations has the potential to inform both therapeutic targets and risk-adapted therapy.

Single-cell analyses have emerged as a powerful way to gain information about heterogeneity within cancer cell populations and have illustrated the importance of co-existing diverse genetic, epigenetic or transcriptional subpopulations for treatment response.[19,20] We hypothesized that single-cell transcriptomics would allow to capture leukemia-intrinsic and immune microenvironmental differences in pathways associated with drug resistance between leukemia and normal immune cells from poverty-exposed and unexposed children with ALL. To address these hypotheses, we employed full-length single-cell RNA sequencing (RNA-seq) of leukemic blasts and microenvironmental cells from poverty-exposed and unexposed children with B-cell ALL (B-ALL). Notably, we identified several differentially enriched pathways in leukemia cells from poverty-exposed patients including steroid responsiveness and signatures consistent with altered immune responses in the leukemia microenvironment that may be associated with treatment resistance.

Methods

Patient samples

Banked diagnostic bone marrow samples from children with *de novo* B-ALL diagnosed between 2005 and 2018, who had consented to biobanking for future research (Dana-Farber Cancer Institute [DFCI] protocols 06-078, 05-001 [*clinicaltrials gov. Identifier: NCT00400946*], 11-001 [*clinicaltrials gov. Identifier: NCT01574274*]) were utilized in this analysis. Parent-reported socioeconomic data from concurrent poverty-focused research protocols (DFCI 11-198 and 16-544) were utilized to annotate biospecimens. Patient demographics and tumor characteristics (immunophenotype, cytogenetics, targeted DNA sequencing) were abstracted from study data and the electronic medical record. This study was approved by the DFCI Institutional Review Board.

Poverty exposure

Poverty was the primary exposure of interest and was defined *a priori* at the household-level utilizing both income-poverty and unmet resource needs. Specifically, patients were considered poverty-exposed if they had concurrent parent reported low-income (annual household income <200% of the Federal Poverty Level [FPL] and household material hardship [HMH] (food, housing, or transportation insecurity) at time of diagnosis. Those with reported income >200% FPL were considered unexposed, regardless of whether HMH data were available.

Cohort assembly

We excluded biospecimens from patients with high-risk immunophenotypic or genetic abnormalities at diagnosis including T-cell immunophenotype, *KMT2A* or *BCR-ABL1* gene rearrangements, or high-risk cytogenetic abnormalities (low hypodiploidy; t[17;19], iAMP21). Analytic specimens were restricted to lymphoblasts with B-cell immunophenotype, *ETV6::RUNX1* translocations or a hyperdiploid karyotype, two genetic features frequently associated with standard risk prognosis, or normal fluorescense *in situ* hybridization (FISH) and cytogenetic testing. Biospecimens were analyzed in a de-identified fashion.

Flow cytometry

Peripheral blood mononuclear cells (PBMC) were isolated using Ficoll-Paque PLUS from GE Healthcare according to the manufacturer's protocol. Samples were stained for CD45-FITC, CD3-PerCP-Cy5.5, CD14-APC-Cy7, CD19-PE, and DAPI (1 μg/mL, Sigma Aldrich) to exclude dead cells. Single cells were sorted into 96-well plates containing TCL buffer (Qiagen) using a Sony SH800 sorter. Minipools of 100 leukemic cells from each patient were sorted in the same way and used for bulk RNA-seq. The number of sorted and sequenced cells per sample are listed in *Online Supplementary Table S4*.

Single-cell RNA sequencing library preparation and sequencing

Full-length single-cell RNA-seq libraries were prepared using the SMART-seq2 protocol.[21] Libraries were pooled and quantified using Qubit dsDNA High Sensitivity reagents. Paired-end sequencing was performed on a NextSeq 500 (Illumina instrument) targeting a sequencing depth of 1 million reads per single cell. Sequencing reads were trimmed using trimmomatic and aligned to the hg19 version reference genome using STAR aligner.[22] Raw counts and normalized TPM values were quantified using HTSeq and RSEM, respectively. Detailed library preparation protocols are provided in the *Online Supplementary Appendix*.

Statistical analysis

All statistical analyses were conducted using R (version 4.0.4) and R packages available at BioConductor. *P* values were adjusted for false discovery rate (FDR) across all comparisons using Holm-Bonferroni. An adjusted *P* value equal or lower than 0.05 and a $\log_2$-fold change of more or equal to 0.58 were considered significant. A parametric

student's *t* test or one-way ANOVA were used to compare means of two groups or multiple groups, respectively. All data represent mean ± standard deviation (SD). *P<0.05; **P<0.01; ***P<0.001; ****P<0.0001, were considered statistically significant.

Results

Single-cell transcriptomic profiling delineates malignant from normal cells in low-risk pediatric B-cell acute lymphoblastic leukemia

We assembled a cohort of poverty-exposed (N=7) (defined as both parent-reported low-income [annual household income <200% FPL] and at least 1 unmet basic resource need [HMH; food, utility or housing insecurity) and unexposed (N=7) children with *de novo* B-ALL who had consented to biobanking of diagnostic bone marrow specimens to assess transcriptional profiles of lymphoblasts and microenvironmental cell populations at diagnosis. To minimize heterogeneity, we excluded patients with high-risk immunophenotype, *KMT2A* or *BCR-ABL1* gene rearrangements, or high-risk cytogenetic abnormalities (low hypodiploidy; t(17;19); iAMP21). The remaining biospecimens included B-cell immunophenotype, *ETV6::RUNX1* translocations or hyperdiploid karyotypes - two genetic features frequently associated with standard-risk prognosis. Clinical, immunophenotype and molecular characteristics are listed in Table 1.

We enriched for leukemia cells from bone marrow by sorting on $CD45^{low}$-expressing blasts and also collected normal T cells, B cells, and myeloid cells by sorting on appropriate surface markers ($CD45^{high}$ $CD3^{+}$ T cells, $CD45^{high}$ $CD19^{+}$ B cells, $CD45^{high}$ $CD14^{+}$ myeloid cells; Figure 1A; see methods). Percentage of each sorted cell type is listed in *Online Supplementary Table S4*.

After single-cell sorting, we performed full-length single-cell transcriptome analysis of 3,166 malignant (852 "poverty-exposed" and 936 "unexposed") and 1,378 normal immune cells (T cells, B cells and myeloid cells) using the Smartseq2 protocol for full-length RNA-seq[21] (*Online Supplementary Figure S1*). For comparison, we also included normal donor cells from six normal donors from published datasets in our analyses (GSE16191, GSE162337).[20,23] As

Table 1. Sociodemographic, clinical, and molecular characteristics at time of diagnosis for N=14 children with standard-risk *de novo* B-cell acute lymphoblastic leukemia.

Sample number	Sex	Age at diagnosis, years	Source	*ETV6::RUNX1*	Cytogenetics	HMH	Income, $ K	% FPL
Unexposed 1	F	4	BM	Neg	High hyperdiploid	No	350	>200
Unexposed 2	M	3	BM	Neg	High hyperdiploid	No	100	>200
Unexposed 3	M	15	BM	Neg	Unremarkable	Unknown	125	>200
Unexposed 4	F	3	BM	Neg	High hyperdiploid	Unknown	200	>200
Unexposed 5	F	2	BM	Pos	Unremarkable	Unknown	113	>200
Unexposed 6	M	4	BM	Pos	Unremarkable	Unknown	150	>200
Unexposed 7	F	2	BM	Neg	High hyperdiploid	Unknown	200	>200
Poverty-exposed 1	M	2	BM	Pos	Unremarkable	Yes	6	<200
Poverty-exposed 2	M	2	BM	Neg	High hyperdiploid	Yes	7	<200
Poverty-exposed 3	M	15	BM	Neg	Failed	Yes	14	<200
Poverty-exposed 4	M	3	BM	Pos	Unremarkable	Yes	0	<200
Poverty-exposed 5	M	2	BM	Pos	Unremarkable	Yes	10	<200
Poverty-exposed 6	F	5	BM	Neg	High hyperdiploid	Yes	21	<200
Poverty-exposed 7	M	3	BM	Pos	Unremarkable	Yes	10	<200

Poverty was defined *a priori* as both parent-reported low-income (annual household income <200% Federal Poverty Level [FPL]) and the presence of household material hardship ([HMH]; food, housing, or utility insecurity). BM: bone marrow; f: female; K: thousand; m: male; neg: negative; pos: positive.

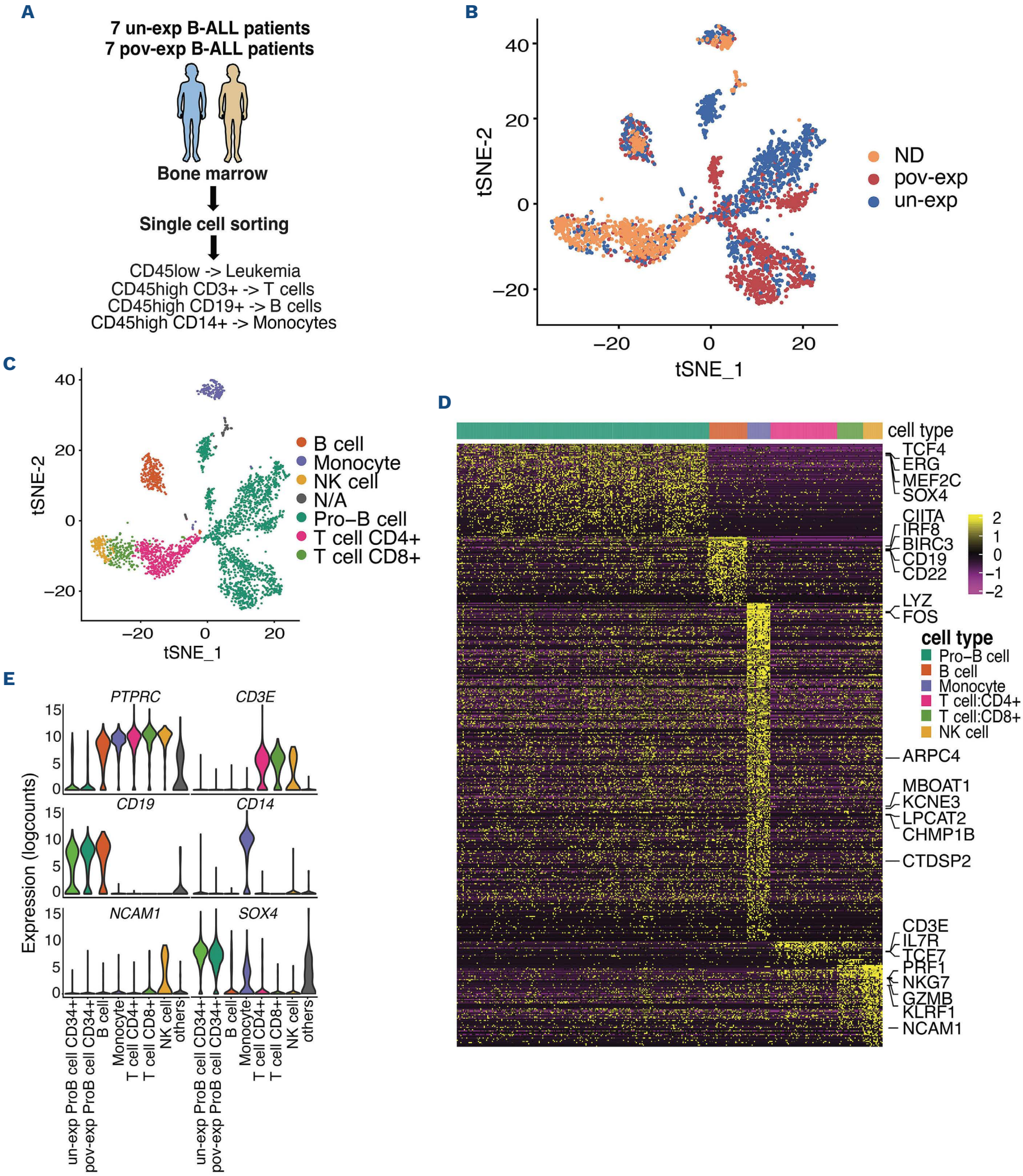

Figure 1. Single-cell transcriptome analysis of pediatric B-cell lymphoblastic leukemia in poverty-exposed *versus* unexposed children. (A) Schematic representation depicting the cohort, sample collection, processing, and sorting of cells for single-cell transcriptional profiling using SMART-seq2 protocol. (B) t-stochastic network embedding (t-SNE) clustering of single-cell gene expression. (C) t-stochastic network embedding (t-SNE) clustering of single-cell gene expression colored by cell type (human cell atlas). (D) Expression of marker genes for each cell type is depicted as a heatmap. (E) Violin plots of canonical marker genes for white blood cells (CD45^{+}), T cells, B cells, monocytes, natural killer (NK) cells, and B-cell lymphoblastic leukemia (B-ALL). ND: normal donor; N/A: not applicable; pov.-exp.: poverty-exposed, un-exp.: unexposed.

these normal donors were all from adult individuals, we verified that main cell types and proportions were similar for pediatric individuals by comparing with public pediatric datasets downloaded from GSE132509 (*Online Supplementary Figure S2*).[24]

After several single-cell RNA-seq quality control filtering steps (see Methods and *Online Supplementary Figure S1*), we performed t-stochastic network embedding (t-SNE)[25] and graph-based clustering from Seurat package to explore cellular compositions, which revealed 17 distinct cell clusters (*Online Supplementary Figure S3A*). Seven clusters (clusters 4, 7, 8, 10, 11, 15 and 16) were shared between patients and normal donors, thus presumably representing normal immune cells, whereas the remaining clusters (1, 2, 5, 9, 13, 14, and 17) were specific to B-ALL patients. Lineage annotation of the single-cell profiles with singleR[26] based on BLUEPRINT[27] and Human Cell Atlas datasets[28,29] revealed that shared clusters indeed represented $CD4^+$ T cells, $CD8^+$ T cells, NK cells, B cells, and myeloid cells, respectively; whereas leukemic cells fell into clusters annotated as Pro-B cells, consistent with their developmental state (Figure 1C; *Online Supplementary Figure S3B*). Additionally, differential expression analysis of well-established canonical lineage marker genes distinguished normal from leukemic clusters (Figure 1D, E). For example, leukemic clusters 1, 2, 5, 9, 13, 14 and 17 expressed *TCF4*, *ERG*, *MEF2C* and *SOX4*, all of which are transcription factors with known function in B-ALL.[30-32] Cluster 4 contained B cells as demonstrated by expression of *IRF8, CIITA, BIRC3, CD19* and *CD22*. T cells localized into clusters 3, 7, and 10 with strong expression of *IL7R, CD3G, CD3D,* and *TCF7*. Cluster 8 contained myeloid cells that express *LYZ* and *FOS*. NK cells with expression of the NK markers *NKG7*, *PRF1* and *GZMB* were found in cluster 11 (Figure 1 D, E; *Online Supplementary Figure S3A*).

To ensure that clusters 1, 2, 5, 9, 13, 14, and 17 were indeed malignant, we called arm level copy number variations (CNV) in normal and presumed malignant clusters using InferCNV (see methods). CNV were limited to leukemic clusters, with copy number events being most prominent in hyperdiploid B-ALL samples (*Online Supplementary Figure S4*).

Leukemia cells fall into distinct clusters based on underlying genetic characteristics and poverty exposure

Interestingly, while some leukemic clusters were patient-specific, other clusters contained cells of several patients (Figure 1B, C). To understand leukemic cluster formation, we first tested whether underlying genetic events might be causal for cluster formation. Leukemic cells that were hyperdiploid or carried *ETV6::RUNX1* translocations clustered separately in t-SNE (Table 1; Figure 2A). Aberrant developmental hierarchies have been described in many cancers including in acute leukemia and have been associated with treatment failure.[19] To address whether leukemic cells from poverty-exposed or unexposed patients may demonstrate aberrant differentiation states, we performed Louvain clustering[33] focusing on genes involved in hematopoietic progenitor and B-lymphoid differentiation using validated signatures from the Human Cell Atlas (*Online Supplementary Table S1*; see methods). This analysis revealed seven clusters (Figure 2B). Leukemia cells from poverty-exposed patients were enriched in clusters 3, 4, 5, 7 while leukemic cells from unexposed patients dominated in clusters 1, 2 and 6 (Figure 2C, D). Of note, all seven clusters contained cells from both genetic subtypes, even though some were enriched in cells from either hyperdiploid or *ETV6::RUNX1* translocated leukemias (i.e., clusters 2 and 4 enriched in hyperdiploid, clusters 3 and 5 enriched in *ETV6::RUNX1* translocated specimens (*Online Supplementary Figure S5A-D*), suggesting that genetic events alone were not solely responsible for cluster formation (*Online Supplementary Figure S5C, D*).

To further characterize these clusters, we performed marker gene and gene set enrichment analysis, comparing clusters enriched in poverty-exposed to those enriched in unexposed specimens. Notably, clusters enriched in poverty-exposed leukemic cells (clusters 3, 4, 5 and 7) demonstrated expression of genes with known relation to treatment response in B-ALL, including genes associated with hematopoietic progenitors (*FOXO1, SMARCA4, JUN, ARID5B, STAG3* and *NPY*), resistance to vincristine (*SOX11, DSC2, KCNN1 ABHD3,* and *MTF2*), and glucocorticoid therapy (*SSPB2, PCNA, IGLL1, ADGRAA3, STMN1* and *PCCA*). In contrast, clusters enriched in unexposed leukemic cells (clusters 1, 2, and 6) were characterized by expression of signatures related to metabolism (*PSAP, COTL2, LOW, CYBB, GLIPR1, ALDH3B1, MTHFD1*) and immune activation (*CD74, ISG20, GBP4*, and *PSME2*) (Figure 2E; *Online Supplementary Table S2*). These analyses reveal distinct heterogenous signatures related to inflammation, metabolism and treatment resistance differentially expressed in leukemic cells from poverty-exposed *versus* unexposed patients.

In further analyses, we collapsed expressed genes of all signatures enriched in poverty-exposed single-cell clusters or unexposed single-cell clusters, respectively, and computed an average expression score (see Methods; *Online Supplementary Table S3*). We then assessed the expression of the poverty-exposed and unexposed signatures among patients who had either *ETV6::RUNX1* translocated or hyperdiploid B-ALL, respectively. Notably, expression of the poverty-exposed signature was higher in poverty-exposed patients within both groups (*Online Supplementary Figure S6A, B*).

We next evaluated whether these signatures might also be differentially expressed in bulk RNA-seq of leukemic cells from poverty-exposed and unexposed patients. To this end, we generated bulk RNA-seq data of the same seven poverty-exposed and seven unexposed patients on whom we had performed single-cell transcriptome analysis. Indeed, poverty-exposed signatures were enriched in the poverty-exposed cohort compared to the unexposed

cohort, whereas the unexposed signatures were enriched in the unexposed compared to the poverty-exposed cohort (Figure 2F). We observed a similar trend when analyzing *ETV6::RUNX1* translocated and hyperdiploid samples separately (*Online Supplementary Figure S6C, D*). We confirmed this trend using CIBERSORTx[34] for deconvolution. Although poverty-exposed signatures were detected in all patients, they were enriched in the poverty-exposed cohort, whereas unexposed signatures were enriched in the unexposed cohort (*Online Supplementary Figure S7*).

We next investigated how these signatures performed in an independent dataset from our institution. To this end,

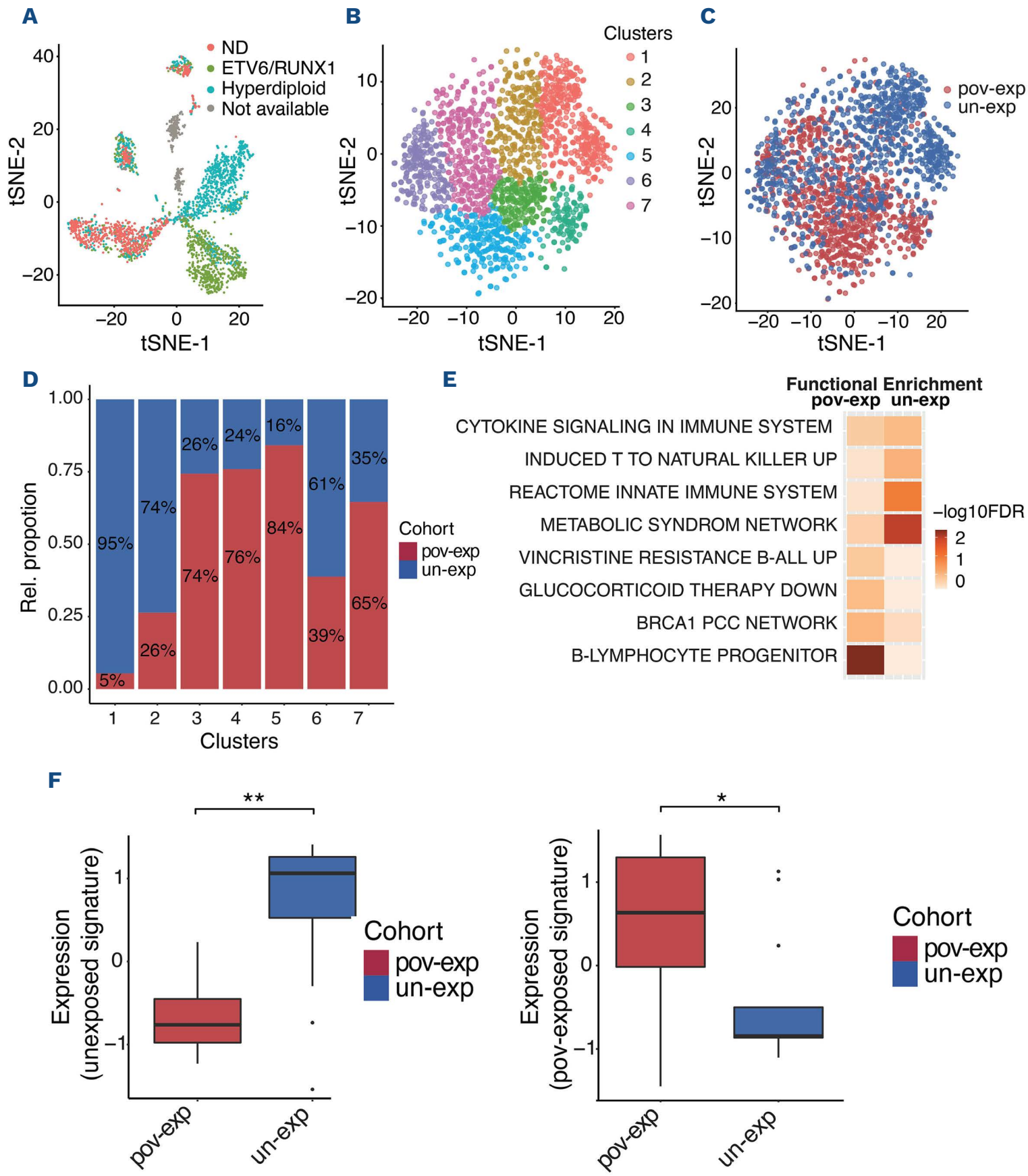

Figure 2. Leukemia blasts from poverty-exposed pediatric B-cell lymphoblastic leukemia patients carry distinct transcriptome features. (A) t-stochastic network embedding (t-SNE) annotated by known cytogenetic abnormalities. (B) t-SNE plot of malignant cells clustered based on expression of known progenitor and lymphoid differentiation signatures (see methods). (C) t-SNE annotated by poverty exposure. (D) Stacked bar plot depicts relative percentage of single leukemic cells from poverty-exposed (pov.-exp.) and unexposed (un-exp.) patients. (E) Gene set enrichment analysis comparing clusters enriched in single cells from pov.-exp. or un-exp. patients (pov.-exp.: clusters 3, 4, 5 and 7; un-exp.: clusters 1, 2, and 6). (F) Expression of pov.-exp. and un-exp. signatures (see methods) in bulk RNA sequencing (N=14; **P*<0.05; ***P*<0.01 by Wicoxon rank test). ND: normal donor.

we analyzed public bulk RNA-seq data downloaded from GSE181157[35] for which we had poverty-exposure annotation (*Online Supplementary Table S5*). The poverty-exposed signature was anti-correlated with the unexposed signature and higher expressed in poverty-exposed patients compared to unexposed patients (*Online Supplementary Figure S8*; see methods).

Taken together, these analyses suggest that leukemia-intrinsic transcriptional circuits differ in diagnostic B lymphoblasts from poverty-exposed children compared to unexposed children with enrichment of signatures associated with drug resistance in poverty-exposed children.

Modulation of myeloid microenvironment in poverty-exposed children with B-cell acute lymphoblastic leukemia

Chronic inflammation has been implicated in adverse outcomes associated with low-socioeconomic status in several childhood diseases, including asthma and obesity.[36,37] To investigate whether the observed differences in inflammatory signatures in leukemic blasts from poverty-exposed *versus* unexposed B-ALL patients might be associated with changes in the immune microenvironment, we identified the composition and transcriptional landscape of the leukemia microenvironment in the same cohort of patients, focusing on B cells, T cells, and myeloid cells as well-defined immune cells. There was no difference in immune cell population frequency between poverty-exposed or unexposed patients (*Online Supplementary Table S4*).

Non-classical monocytes expressing CD16 (FCGR3A) have recently been shown to be enriched in B-ALL at time of diagnosis and at relapse.[38] Indeed, transcriptional analysis revealed that while normal donor myeloid cells strongly express *CD14*, myeloid cells from B-ALL patients, expressed lower levels of *CD14* with concurrently higher expression of *CD16* (*FCGR3A*) (Figure 3A, left). Notably, myeloid cells from unexposed patients showed stronger expression of *CD16* (*FCGR3A*) than those from poverty-exposed patients (Figure 3A, right). This trend was also present when analyzing samples from *ETV6::RUNX1* translocated patients separately from hyperdiploid samples (*Online Supplementary Figure S9A*).

To further investigate possible transcriptional differences in myeloid cells from poverty-exposed and unexposed leukemia patients, we employed SC3 clustering[39] (see methods) and identified five myeloid clusters (*Online Supplementary Figure S9B*), with cluster 1 being dominated by normal donor myeloid cells (*Online Supplementary Figure S9B, C*). Interestingly, while the remaining four clusters contained mostly myeloid cells from leukemic patients, clusters 2 and 4 were dominated by unexposed patients, whereas cluster 3 was enriched in myeloid cells from poverty-exposed patients (*Online Supplementary Figure S9B, C*). To further characterize these clusters, we first looked at validated myeloid expression signatures, including expression signatures for classical monocytes (Mono1), and non-classical monocytes (Mono2).[40] As expected, cluster 1, which contained the largest fraction of normal donor myeloid cells showed strong expression for the classical monocyte signature Mono1 (*Online Supplementary Figure S9D*). Cluster 2 (enriched in unexposed patients) was dominated by expression of the non-classical monocyte signature Mono2 and likely represents non-classical monocytes that had been previously shown to be enriched in B-ALL.[38] In contrast, clusters 3 (enriched in poverty-exposed patients) and 4 (enriched in unexposed patients) demonstrated expression of classical monocyte signatures, but in addition expressed the Mono3 signature (associated with differentiation and trafficking in cycling monocytes),[41] and Mono4 signature (associated with cytotoxicity),[40] respectively (*Online Supplementary Figure S9D*). Cluster 5, which consists of poverty-exposed and unexposed myeloid cells, did not show strong enrichment for any of the four monocyte signatures.

To further characterize differences between these clusters, we performed marker gene and gene set enrichment analysis (Figure 3B, C; *Online Supplementary Table S3*). This analysis confirmed that genes associated with classical monocytes such as *TREM1, CD163, ALDH1A1, NLRP3, LYZ,* and *PLD3* were strongly expressed in cluster 1. Cluster 2 expressed the non-classical monocyte signature genes *CX3CR1, SIGLEC10* and *CYTIP*, and in addition expressed genes involved in inflammatory response (*FCGR3A, SAT1, GCH1, LYN,* and *LST1*), immune regulation (*LILRB2, IFITM1, PILRA, ITGAL* and *ICAM2*), and cytotoxicity (*FCGR3B, TNF, FCER1G,* and *PTPN6*). Interestingly, myeloid cells in cluster 3 - which were enriched in poverty-exposed patients - expressed signatures associated with cytokine signaling (*IL1B, SOCS3, TNFRSF1A, IL4R, SELL, IL4R* and *IL6R*), complement (*CD55, CLU, GCA* and *S100A12*), and reactive oxygen species pathway (*PRDX1, TXN* and *FES*). In contrast, cluster 4, enriched in myeloid cells from unexposed patients was enriched for genes associated with interferon α and β signaling (*OAS3, OAS1, STAT2, MX2, RSAD2* and *PARP9*). Lastly, cluster 5, shared by both poverty-exposed and unexposed patients, demonstrated enrichment in interferon γ response, but to lesser extent than cluster 4 (*LCP2, STAT1, IFI44,* and *ISG15*).

Signaling alterations in myeloid cells have been associated with response to social adversity.[42,43] To evaluate whether similar mechanisms may be at play in pediatric leukemia patients we assessed expression of the conserved transcriptional response to adversity (CTRA).[44] Indeed, we observed higher expression of the inflammatory CTRA signature in myeloid cells from patients exposed to poverty compared to unexposed which showed higher expression of the interferon CTRA signature (Figure 3D; see methods).

These findings indicate that myeloid cells from children exposed to poverty exhibit altered immune responses including expression of the inflammatory CTRA signature previously described in health adversity.

Alterations in T- and B-cell profiles among poverty-exposed children with B-cell lymphoblastic leukemia

We next explored differences in mature lymphoid cell composition between poverty-exposed and unexposed B-ALL patients. Overall percentages of B cells, $CD4^+$ and $CD8^+$ T cells from leukemia patients were comparable to normal donor and did not differ between poverty-exposed and unexposed patients (*Online Supplementary Table S4*).

To explore if B-cell subtypes might differ between poverty-exposed and unexposed patients, we clustered B cells using Louvain clustering in t-SNE space and identified five clusters (Figure 4A, B). SingleR annotation using validated human cell atlas annotations showed that these clusters included mostly naïve, immature and memory B cells, respectively, with clusters 2 and 4 being enriched in naïve B cells, and clusters 1 and 5 in memory B cells (Figure 4C). Notably, while cluster 2 representing naïve B cells was enriched in normal donor B cells, the remaining clusters contained B

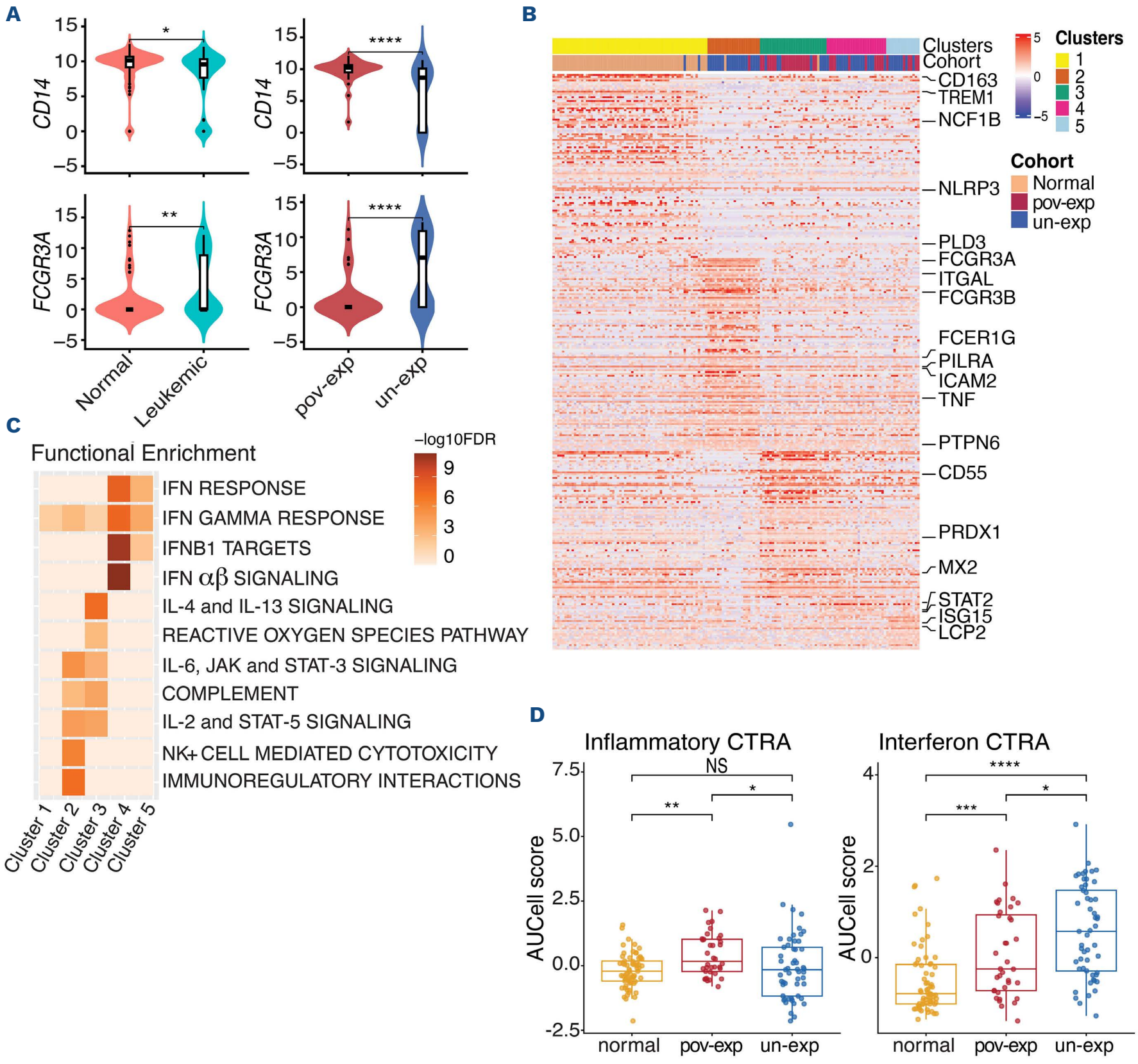

Figure 3. Distinct monocyte population in poverty-exposed versus unexposed patients. (A) Violin plots demonstrating expression of *CD14* and *CD16* (FCGFR3A) in normal donor (normal), monocytes from leukemia patients or poverty-exposed and unexposed patients, respectively (**P*<0.05; ***P*<0.01; *****P*<0.0001 by two-sided Wilcoxon test). (B) Heatmap depicting the expression of marker genes per cluster. (C) Functional enrichment of different clusters using gene set enrichment analysis (see methods). (D) Box plots showing expression of inflammatory and interferon conserved transcriptional response to adversity signatures (****P*<0.001 by two-sided Wilcoxon test). FDR: false discovery rate; NS: not significant.

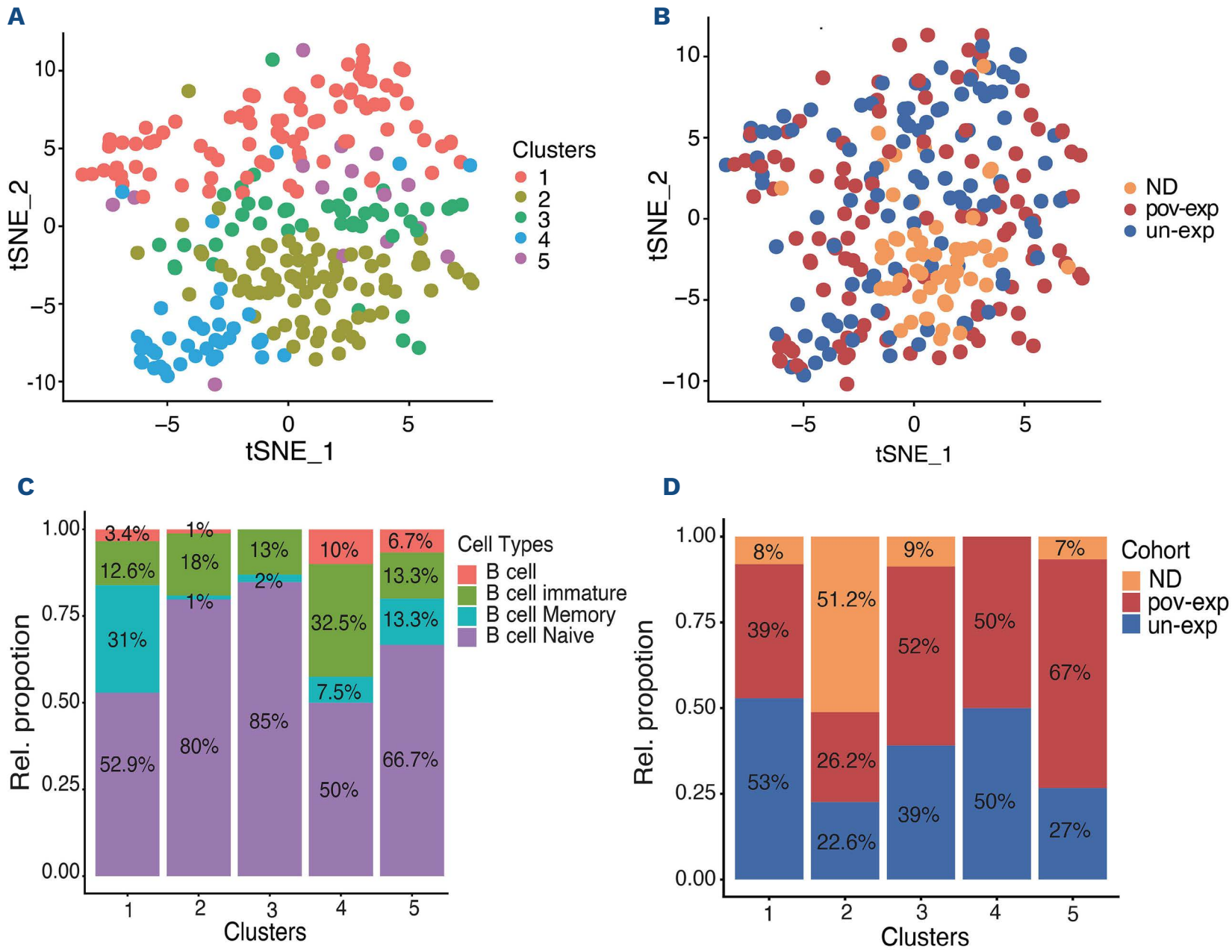

Figure 4. B-cell populations in poverty-exposed and unexposed children with B-cell lymphoblastic leukemia compared to normal donors. (A) t-stochastic network embedding (t-SNE) plot depicting 5 B-cell clusters by Louvain clustering. (B) t-SNE plot depicting distribution of B cells from normal donors (ND), poverty-exposed (pov.-exp.) and unexposed (un-exp.) children with B-cell lymphoblastic leukemia (B-ALL). (C) Bar plot depicting relative proportions of B-cell subtypes as annotated by human cell atlas per cluster. (D) Bar plot depicting relative proportions of B cells from ND, pov.-exp. andun-exp. children with B-ALL across 5 clusters.

cells from both poverty-exposed and unexposed patients (Figure 4D). We were also unable to detect differences when analyzing samples from *ETV6::RUNX1* translocated patients separately from hyperdiploid patients, albeit these analyses are limited by the small sample size (*Online Supplementary Figure S10A-D*). Thus, representation of B-cell subsets was overall similar between poverty-exposed and unexposed patients with B-ALL.

Next, we focused on T cells and first separated CD4$^+$ from CD8$^+$ T cells using validated human cell atlas annotations (Figure 5A). We then performed Louvain clustering of CD4$^+$ annotated T cells and identified 4 clusters (Figure 5B; *Online Supplementary Figure S11A*). Further annotation using singleR, marker gene and gene set enrichment analysis demonstrated that cluster 1 was dominated by CD4$^+$ central memory cells, clusters 2 and 3 consisted of naïve CD4$^+$ T cells, and cluster 4 contained effector memory CD4$^+$ T cells (Figure 5C, D). While normal donor T cells were enriched in cluster 1, all CD4$^+$ T-cell clusters contained cells from poverty-exposed and unexposed B-ALL patients. Poverty-exposed patients demonstrated slightly higher frequencies of CD4$^+$ T cells in clusters 2 and 3, while unexposed patients contained slightly more cells in cluster 4 (Figure 5E). While overall percentages of CD4$^+$ T cells were comparable, poverty-exposed patients demonstrated relatively more naïve and central memory CD4$^+$ T cells and fewer effector memory CD4 T cells (*Online Supplementary Figure S11B*). We detected similar differences when analyzing samples from *ETV6::RUNX1* translocated patients separately from hyperdiploid patients, with the caveat that these analyses are limited by the small sample size (*Online Supplementary Figure S11C-F*).

CD8$^+$ T cells separated into two clusters by Louvain clustering (Figure 6A), with cluster 1 containing higher

frequencies of CD8⁺ T cells from unexposed patients, and cluster 2 being enriched in CD8⁺ T cells from poverty-exposed patients (Figure 6B). By marker gene analysis, cells in cluster 1 expressed genes associated with T-cell activation and dysfunction including *GZMA, GMZB, PRF1, TIGIT* and *IL10RA*, whereas cluster 2 cells expressed genes associated with naïve or central memory T cells, such as *CCR7, TCF7, LEF1* and *SELL* (Figure 6C). We next computed the average expression of genes that have been previously validated as expressed in naïve, cytotoxic, and dysfunctional T cells

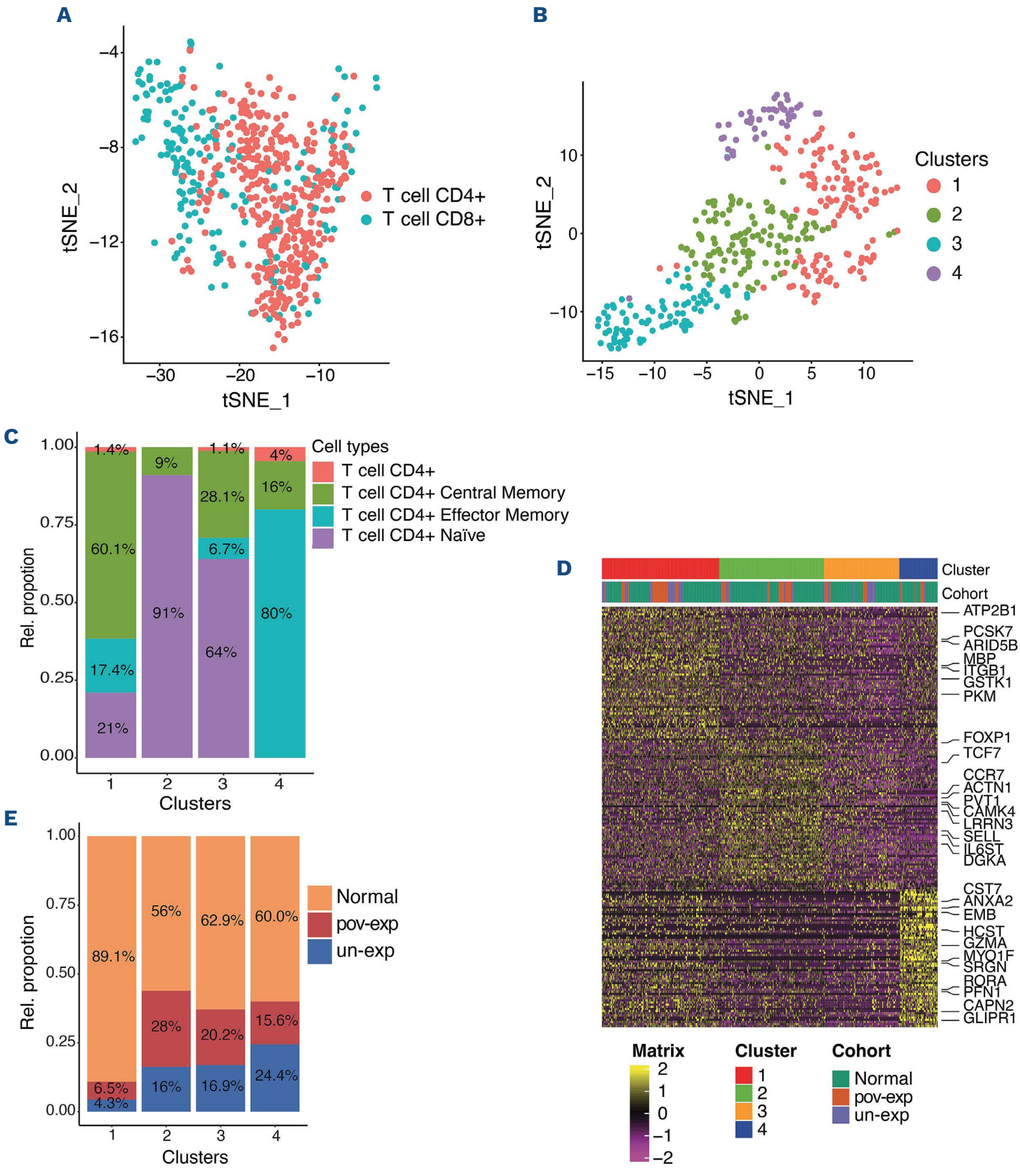

Figure 5. CD4⁺ T-cell populations in poverty-exposed and unexposed children with B-cell lymphoblastic leukemia compared to normal donors. (A) t-stochastic network embedding (t-SNE) plot depicting T cells annotated as CD4⁺ or CD8⁺ T cells (human cell atlas), respectively. (B) t-SNE of CD4⁺ T cells separating into 4 clusters by Louvain clustering. (C) Bar plot depicting relative proportions of CD4⁺ T-cell subtypes as annotated by human cell atlas. (D) Heatmap depicting expression of marker genes of CD4⁺ T cells per cluster. (E) Bar plot depicting relative proportions of CD4⁺ T cells from normal donors (ND), poverty-exposed (pov.-exp.) and unexposed (un-exp.) children with B-cell lymphoblastic leukemia (B-ALL) across 4 clusters.

(see methods). The cytotoxic signature was expressed at a higher level in cluster 1 compared to cluster 2, whereas the naïve and exhausted signature was higher expressed in cluster 2 (Figure 6D). Thus, these analyses point towards an imbalance of naïve, activated, and dysfunctional T cells in poverty-exposed patients that are enriched in cluster 2 compared to T cells from unexposed patients which were preferentially enriched in cluster 1.

Discussion

Using single-cell RNA-seq of leukemic blasts and their immune microenvironment in a cohort of children with B-ALL, we identified several differentially enriched pathways in leukemia cells from poverty-exposed and unexposed patients including steroid responsiveness and signatures consistent with altered immune responses in the leukemia

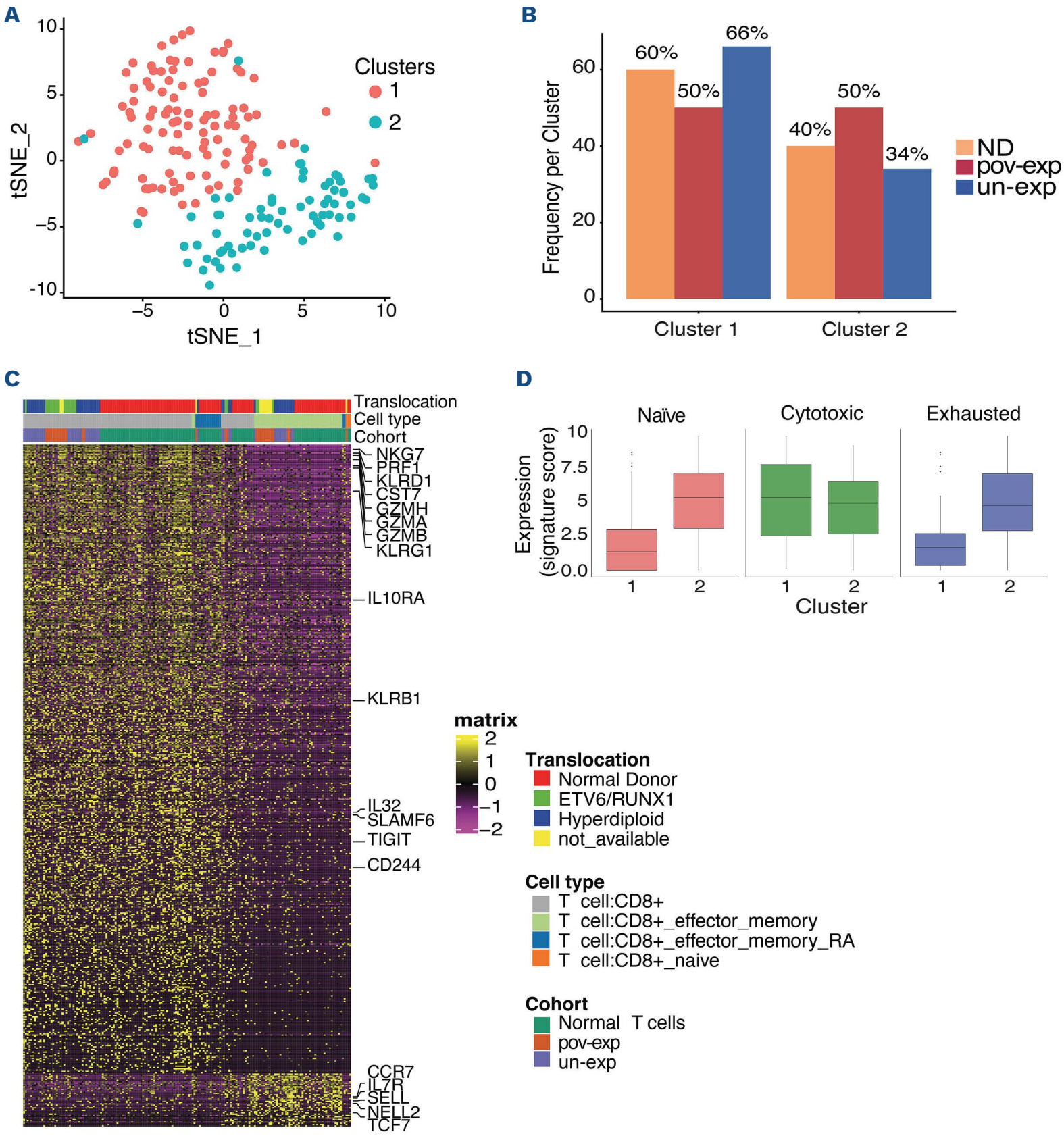

Figure 6. Distinct CD8⁺ T-cell subpopulations in poverty-exposed compared to unexposed children with B-cell lymphoblastic leukemia. (A) t-stochastic network embedding (t-SNE) plot of CD8⁺ T cells separating into 2 clusters by Louvain clustering. (B) Bar plot depicting relative proportions of CD8⁺ T cells from normal donors (ND), poverty-exposed (pov.-exp.) and unexposed (un-exp.) children with B-cell lymphoblastic leukemia (B-ALL) across 2 clusters. (C) Heatmap depicting marker gene expression of CD8⁺ T cells per cluster. (D) Gene expression signature scores for naïve, cytotoxic and exhaustion CD8⁺ T cells in cluster 1 *versus* cluster 2 (see methods).

microenvironment that may be associated with treatment resistance.

These data point toward several potential mechanisms of adverse treatment response that may explain observed disparities in relapse and survival among children with B-ALL living in poverty. First, our data suggest that poverty-exposed patients with B-ALL have fewer leukemia cells susceptible to steroids at diagnosis. Steroids are a core component of ALL chemotherapy and poor response to steroids is a well-accepted mechanism of treatment failure in ALL.[45] Poverty exposure is associated with "toxic stress," defined by the National Research Council as the excessive activation of stress regulatory systems in the absence of adequate buffering.[14] Toxic stress physiology includes dysregulation of the hypothalamic-pituitary-adrenocortical axis and the sympathetic-adrenomedullary system that result in perturbations in stress hormones, elevated inflammatory cytokine responses, and altered cellular metabolism.[14,16,46] It is intriguing to speculate that elevated levels of endogenous cortisol may potentially contribute to inherent steroid resistance of leukemic blasts. Notably, prior studies in adult acute myeloid leukemia patients with low SES undergoing hematopoietic stem cell transplantation have demonstrated higher expression of glucocorticoid receptor signaling signatures in PBMC pre-transplant compared to non-exposed patients.[47]

Prior studies have demonstrated the co-existence of toxic stress and chronic inflammation in asthma, cardiovascular disease, and depression, among other chronic diseases,[10,13,14] yet it is unknown how this might affect the development of cancer or its immune surveillance. Related, prior work in solid tumor mouse-models suggest that interventions targeting adrenergic receptor responses of the microenvironment - such as β-blockade - may impact chemotherapy responsiveness.[49]

Inflammatory signatures in tumor cells, including leukemias, have been linked to inferior treatment response - hypothesized to be due in part to immune dysfunction in the tumor microenvironment that prevents a host-immune response against the tumor.[48,49] Mechanisms of immune dysfunction are well established in many solid tumors and emerging data suggest an important role for aberrant immune activation in ALL.[20,48] There is sparse knowledge with regards to the composition and functional characteristics of the tumor immune microenvironment among patients who experience poverty and other adverse social determinants of health. Our results point towards unique immune derangements that occur in children with B-ALL in the context of poverty exposures, notably an increased expression of inflammatory signatures in myeloid cells and an imbalance of CD8 naïve and effector cells. Importantly, myeloid cells from poverty-exposed B-ALL patients also express inflammatory signatures that have previously been associated with adversity in other disease contexts,[42,43] arguing that these alterations might represent universal changes that occur in the setting of hardship and may offer unique therapeutic possibilities. For example, interventions targeting adrenergic receptor responses through β-blockade have been shown to reduce chemotherapy resistance in select solid tumors,[50] yet possible effects on the immune microenvironment have not been explored.

It is notable that one in three children with ALL is exposed to poverty at the time of diagnosis,[3] and these children are more likely to experience early relapse of their disease. Consequently, our data highlighting potential mechanisms of treatment resistance in the context of poverty-exposure hold immediate relevance for a third of children with the most common pediatric cancer diagnosis - a number far higher than any high-risk ALL genomic alteration. Specifically, further work to clarify associations between poverty-exposure, steroid resistance and immune microenvironment have the potential to be translated to future risk-adapted therapeutic approaches - for example, chemotherapy regimens that are relatively steroid-sparing, or those that directly target the tumor microenvironment to induce or maintain remission. If successful, such risk-adapted approaches to treatment could reduce excess relapse - an outcome to both improve ALL survival and concurrently to reduce the toxicity associated with the treatment of relapsed ALL.

Our data are limited by a small sample size, including seven children in each cohort, and thus exploratory in nature. Future replication of these findings in a larger cohort is necessary and will allow investigation of poverty-associated signatures stratified by genetic sub-type that is not possible in our sample. More detailed studies are needed to better understand the relative contributions of myeloid cells and $CD8^-$ T cells and their interactions with leukemic cells in the context of poverty-exposure employing additional single-cell sequencing approaches that allow profiling of a larger number of cells such as the multimodal approaches available on the 10X platform. Further studies may also shed light on the relative contributions of underlying leukemic genetic events in shaping the leukemia immune microenvironment. Additionally, future studies are needed to determine if the observed leukemia-intrinsic and microenvironmental alterations are limited to children with B-ALL or if they also occur in the setting of genomic high-risk ALL and their relevance for other pediatric cancers.

One in three children with ALL lives in poverty at the time of diagnosis, and these children disproportionately experience treatment failure in the form of early relapse of their disease.[3] Future work to unravel tumor microenvironmental and epigenetic state changes associated with poverty exposure may identify opportunities for therapeutic targeting and resistance-adapted chemotherapy relevant to a strikingly high proportion of children with ALL.

Disclosures

JGL received research funding from Bristol Myers Squibb

for an unrelated project. All other authors have no conflicts of interest to disclose.

Contributions

KB and BK conceptualized and supervised this study. AG-A, EMM, NS, KB, and BK co-wrote the manuscript. AG-A performed experiments and analyzed the data. EMM and NS performed data analysis. AG-A, SP, TV, MN, VD, and JF performed experiments. YP, MH, AEP, and LBS provided clinical samples. JGL provided scientific input for study design and/or data analysis. All authors reviewed and edited the manuscript.

Acknowledgments

We thank the Flow Cytometry Core at Dana-Farber Cancer Institute for their assistance, the Pediatric Oncology Outcomes research team and the Clinical Research Coordinators ALL study team at Dana-Farber Cancer Institute for their help with primary patient samples, and Dr. Judy Ou at Huntsman Cancer Institute for critical comments.

Funding

This work was supported by a Helen Trailblazers Award by Dana-Farber Cancer Institute/Pussycat Foundation (to KB and BK), National Cancer Institute - DF/HCC Nodal Award (2P30CA006516-52) (to KB and BK) and R01CA249185 (to BK), and a Children's Cancer Research Fund award (to BK).

Data-sharing statement

Sequencing data have been deposited in GEO (reference number GSE237888). Codes used for all analyses are available upon request from the corresponding author.

References

1. Bona K, London WB, Guo D, Frank DA, Wolfe J. Trajectory of material hardship and income poverty in families of children undergoing chemotherapy: a prospective cohort study. Pediatr Blood Cancer. 2016;63(1):105-111.
2. Gupta S, Dai Y, Chen Z, et al. Racial and ethnic disparities in childhood and young adult acute lymphocytic leukaemia: secondary analyses of eight Children's Oncology Group cohort trials. Lancet Haematol. 2023;10(2):e129-e141.
3. Bona K, Blonquist TM, Neuberg DS, Silverman LB, Wolfe J. Impact of socioeconomic status on timing of relapse and overall survival for children treated on Dana-Farber Cancer Institute ALL Consortium Protocols (2000-2010). Pediatr Blood Cancer. 2016;63(6):1012-1018.
4. Inaba H, Pui C-H. Advances in the diagnosis and treatment of pediatric acute lymphoblastic leukemia. J Clin Med. 2021;10(9):1926.
5. Ward E, DeSantis C, Robbins A, Kohler B, Jemal A. Childhood and adolescent cancer statistics, 2014. CA Cancer J Clin. 2014;64(2):83-103.
6. Hunger SP, Raetz EA. How I treat relapsed acute lymphoblastic leukemia in the pediatric population. Blood. 2020;136(16):1803-1812.
7. Vrooman LM, Blonquist TM, Stevenson KE, et al. Efficacy and toxicity of pegaspargase and calaspargase pegol in childhood acute lymphoblastic leukemia: results of DFCI 11-001. J Clin Oncol. 2021;39(31):3496-3505.
8. Wadhwa A, Chen Y, Hageman L, et al. Poverty and relapse risk in children with acute lymphoblastic leukemia: a Children's Oncology Group study AALL03N1 report. Blood. 2023;142(3):221-229.
9. Hoppmann AL, Hurley DM, Cramer S, et al. Neighborhood socioeconomic status and overall survival among children with acute lymphoblastic leukemia. Blood Adv. 2025;9(22):5861-5869.
10. Singh GK, Jemal A. Socioeconomic and racial/ethnic disparities in cancer mortality, incidence, and survival in the United States, 1950-2014: Over six decades of changing patterns and widening inequalities. J Environ Public Health. 2017;2017:2819372.
11. Chen E, Miller GE. Socioeconomic status and health: mediating and moderating factors. Annu Rev Clin Psychol. 2013;9:723-749.
12. Adler NE, Newman K. Socioeconomic disparities in health: pathways and policies. Health Aff (Millwood). 2002;21(2):60-76.
13. Braveman P, Gottlieb L. The social determinants of health: it's time to consider the causes of the causes. Public Health Rep. 2014;129 Suppl 2(Suppl 2):19-31.
14. Seeman M, Stein Merkin S, Karlamangla A, Koretz B, Seeman T. Social status and biological dysregulation: the "status syndrome" and allostatic load. Soc Sci Med. 2014;118:143-151.
15. Shonkoff JP. Leveraging the biology of adversity to address the roots of disparities in health and development. Proc Natl Acad Sci U S A. 2012;109 Suppl 2(Suppl 2):17302-17307.
16. Blair C, Raver CC. Poverty, stress, and brain development: new directions for prevention and intervention. Acad Pediatr. 2016;16(Suppl 3):S30-36.
17. Schiavone S, Colaianna M, Curtis L. Impact of early life stress on the pathogenesis of mental disorders: relation to brain oxidative stress. Curr Pharm Des. 2015;21(11):1404-1412.
18. Lupien SJ, McEwen BS, Gunnar MR, Heim C. Effects of stress throughout the lifespan on the brain, behaviour and cognition. Nat Rev Neurosci. 2009;10(6):434-445.
19. van Galen P, Hovestadt V, Wadsworth Ii MH, et al. Single-cell RNA-seq reveals AML hierarchies relevant to disease progression and immunity. Cell. 2019;176(6):1265-1281.e24.
20. Anand P, Guillaumet-Adkins A, Dimitrova V, et al. Single-cell RNA-seq reveals developmental plasticity with coexisting oncogenic states and immune evasion programs in ETP-ALL. Blood. 2021;137(18):2463-2480.
21. Picelli S, Faridani OR, Björklund AK, Winberg G, Sagasser S, Sandberg R. Full-length RNA-seq from single cells using Smart-seq2. Nat Protoc. 2014;9(1):171-181.
22. Dobin A, Davis CA, Schlesinger F, et al. STAR: ultrafast universal RNA-seq aligner. Bioinformatics. 2013;29(1):15-21.
23. Frede J, Anand P, Sotudeh N, et al. Dynamic transcriptional reprogramming leads to immunotherapeutic vulnerabilities in myeloma. Nat Cell Biol. 2021;23(11):1199-1211.
24. Caron M, St-Onge P, Sontag T, et al. Single-cell analysis of childhood leukemia reveals a link between developmental states and ribosomal protein expression as a source of intra-

individual heterogeneity. Sci Rep. 2020;10(1):8079.
25. Kobak D, Berens P. The art of using t-SNE for single-cell transcriptomics. Nat Commun. 2019;10(1):5416.
26. Aran D, Looney AP, Liu L, et al. Reference-based analysis of lung single-cell sequencing reveals a transitional profibrotic macrophage. Nat Immunol. 2019;20(2):163-172.
27. Fernández JM, de la Torre V, Richardson D, et al. The BLUEPRINT data analysis portal. Cell Syst. 2016;3(5):491-495.e5.
28. Hay SB, Ferchen K, Chetal K, Grimes HL, Salomonis N. The Human Cell Atlas bone marrow single-cell interactive web portal. Exp Hematol. 2018;68:51-61.
29. Regev A, Teichmann SA, Lander ES, et al. The human cell atlas. Elife. 2017;6:e27041.
30. Ramezani-Rad P, Geng H, Hurtz C, et al. SOX4 enables oncogenic survival signals in acute lymphoblastic leukemia. Blood. 2013;121(1):148-155.
31. Wu Z, Zhang F, Liu C, et al. Whole transcriptome sequencing reveals a TCF4-ZNF384 fusion in acute lymphoblastic leukemia. Front Oncol. 2022;12:900054.
32. Zhang J, McCastlain K, Yoshihara H, et al. Deregulation of DUX4 and ERG in acute lymphoblastic leukemia. Nat Genet. 2016;48(12):1481-1489.
33. Blondel VD, Guillaume J-L, Lambiotte R, Lefebvre E. Fast unfolding of communities in large networks. J Stat Mech. 2008;2008(10):P10008.
34. Newman AM, Steen CB, Liu CL, et al. Determining cell type abundance and expression from bulk tissues with digital cytometry. Nat Biotechnol. 2019;37(7):773-782.
35. Tran TH, Langlois S, Meloche C, et al. Whole-transcriptome analysis in acute lymphoblastic leukemia: a report from the DFCI ALL Consortium Protocol 16-001. Blood Adv. 2022;6(4):1329-1341.
36. Trivedi M, Denton E. Asthma in children and adults - what are the differences and what can they tell us about asthma? Front Pediatr. 2019;7:256.
37. Furman D, Campisi J, Verdin E, et al. Chronic inflammation in the etiology of disease across the life span. Nat Med. 2019;25(12):1822-1832.
38. Witkowski MT, Dolgalev I, Evensen NA, et al. Extensive remodeling of the immune microenvironment in B cell acute lymphoblastic leukemia. Cancer Cell. 2020;37(6):867-882.e12.
39. Kiselev VY, Kirschner K, Schaub MT, et al. SC3: consensus clustering of single-cell RNA-seq data. Nat Methods. 2017;14(5):483-486.
40. Villani A-C, Satija R, Reynolds G, et al. Single-cell RNA-seq reveals new types of human blood dendritic cells, monocytes, and progenitors. Science. 2017;356(6335):eaah4573.
41. Olingy CE, Dinh HQ, Hedrick CC. Monocyte heterogeneity and functions in cancer. J Leukoc Biol. 2019;106(2):309-322.
42. Taylor MR, Cole SW, Strom J, et al. Unfavorable transcriptome profiles and social disadvantage in hematopoietic cell transplantation: a CIBMTR analysis. Blood Adv. 2023;7(22):6830-6838.
43. Cole SW. The conserved transcriptional response to adversity. Curr Opin Behav Sci. 2019;28:31-37.
44. Knight JM, Rizzo JD, Hari P, et al. Propranolol inhibits molecular risk markers in HCT recipients: a phase 2 randomized controlled biomarker trial. Blood Adv. 2020;4(3):467-476.
45. Pui C-H, Yang JJ, Hunger SP, et al. Childhood acute lymphoblastic leukemia: progress through collaboration. J Clin Oncol. 2015;33(27):2938-2948.
46. Johnson SB, Riley AW, Granger DA, Riis J. The science of early life toxic stress for pediatric practice and advocacy. Pediatrics. 2013;131(2):319-327.
47. Knight JM, Rizzo JD, Logan BR, et al. Low socioeconomic status, adverse gene expression profiles, and clinical outcomes in hematopoietic stem cell transplant recipients. Clin Cancer Res. 2016;22(1):69-78.
48. Witkowski MT, Kousteni S, Aifantis I. Mapping and targeting of the leukemic microenvironment. J Exp Med. 2020;217(2):e20190589.
49. Chu Y, Dai E, Li Y, et al. Pan-cancer T cell atlas links a cellular stress response state to immunotherapy resistance. Nat Med. 2023;29(6):1550-1562.
50. Manoleras AV, Sloan EK, Chang A. The sympathetic nervous system shapes the tumor microenvironment to impair chemotherapy response. Front Oncol. 2024;14:1460493.